Supplementary Information
Supplementary online materials for

Optimization of thermoelectric efficiency in SnTe: The case for the light band

Min Zhou[1, 3,†], Zachary M. Gibbs[2,†], Heng Wang[3], Yemao Han[1], Caini Xin[1], Laifeng Li[1,*], G. Jeffrey Snyder[3,4,*]

1 Key Laboratory of Cryogenics, Technical Institute of Physics and Chemistry, Chinese Academy of Sciences, Beijing 100190, China
2 Division of Chemistry and Chemical Engineering, California Institute of Technology, 1200 E. California Blvd. Pasadena, CA 91125, USA
3 Materials Science, California Institute of Technology, 1200 California Blvd., Pasadena, CA 91125, USA
4 ITMO University, Saint Petersburg Russia

This PDF file includes:
Figure S1, S2, S3, S4, S5
Table S1

† Min Zhou and Zachary M. Gibbs have contributed equally to this work.
* Prof. Laifeng Li, Key Laboratory of Cryogenics, Technical Institute of Physics and Chemistry, Chinese Academy of Sciences, Beijing 100190, China. E-mail: laifengli@mail.ipc.ac.cn
* Dr. G. Jeffrey Snyder, Materials Science, California Institute of Technology, Pasadena, CA 91125, USA. E-mail: jsnyder@caltech.edu

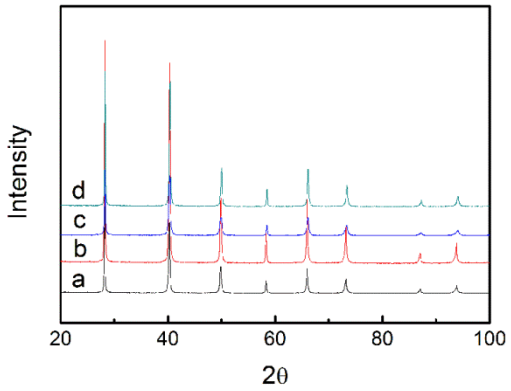

Figure S1. X-ray diffraction patterns of $SnTe_{1-x}I_x$, $SnTe_{1+y}$, and $Gd_zSn_{1-z}Te$ samples with no impurities observed. (a) SnTe, (b) $SnTe_{0.985}I_{0.015}$, (c) $Gd_{0.01}Sn_{0.99}Te$, (d) $SnTe_{1.015}$.

Table S1 A list of samples and some of their room temperature transport properties at 300 K.

Label	Composition	$p_H(10^{19}cm^{-3})$	$\mu_H(cm^2/Vs)$	$\alpha(\mu V/K)$
1E20(SnTe)	SnTe	1.13E20	487	8
1.3E20(0.25% I)	$SnTe_{0.9975}I_{0.0025}$	1.3E20	392	9
9E19(0.5% I)	$SnTe_{0.995}I_{0.005}$	9.2E19	558	8
1.1E20(0.75% I)	$SnTe_{0.9925}I_{0.0075}$	1.1E20	390	11
6E19(1.0% I)	$SnTe_{0.99}I_{0.01}$	6.1E19	545	12
6.3E19(1.25% I)	$SnTe_{0.9875}I_{0.0125}$	6.3E19	430	20
4E19(1.5% I)	$SnTe_{0.985}I_{0.015}$	3.8E19	740	27
3.1E19(2.0% I)	$SnTe_{0.98}I_{0.02}$	3.1E19	460	29
1.3E20(0.3% Te)	$SnTe_{1.003}$	1.3E20	393	10
2E20(0.5% Te)	$SnTe_{1.005}$	2.5E20	222	11
6E20(1.5% Te)	$SnTe_{1.015}$	6.4E20	87	29
1.7E20(0.25% Gd)	$Gd_{0.0025}Sn_{0.9975}Te$	1.66E20	234	8
3E20(0.5% Gd)	$Gd_{0.005}Sn_{0.995}Te$	3.36E20	109	10
4E20(1.0% Gd)	$Gd_{0.01}Sn_{0.99}Te$	3.72E20	89	14
4.4E20(1.5% Gd)	$Gd_{0.015}Sn_{0.985}Te$	4.42E20	72	16
5.0E20(2.0% Gd)	$Gd_{0.02}Sn_{0.98}Te$	4.96E20	61	17

Two-band-modeling details.

It has been found that the minimum of the band gap of SnTe is in the L point of the first Brillouin zone and that there is a second valence band near the first one on the Σ axis[1, 2]. In this paper it was assumed that the light band is nonparabolic and the heavy band is parabolic. Two-band model (SKB modeling for light band and SPB modeling for the heavy band) is applied to explain thermoelectric transport properties.

We consider the Seebeck coefficient of a semiconductor whose electrical conductivity is due entirely to holes which are distributed between two nondegenerate valence bands. It is shown that

the Seebeck coefficient can increase to a maximum with increasing Hall carrier concentration, although the Seebeck coefficient associated with each band decreases in the usual manner with increasing carrier concentration.

The Seebeck coefficient and electrical conductivity of a two band semiconductor are given by:

$$S=(S_L\sigma_L+S_H\sigma_H)/(\sigma_L+\sigma_H),$$

$$\sigma_= \sigma_L+\sigma_H = p_L\mu_Le+p_H\mu_He,$$

Where the subscripts L and H refer to the light-mass valence band and heavy-mass valence band, respectively. And p is the hole concentration, μ is the hole mobility, e is the electron charge. For simplicity, we used the rigid band approximation which assumes that the changing carrier concentration adjusts only the chemical potential position and not the shape or position of the bands.

Within the Kane model, the transport parameters of light band are expressed as follows:

The Seebeck coefficient α_L of light-mass valence band:

$$S_L = \frac{\kappa_B}{e}\left[\frac{{}^1\mathrm{F}^1_{-2}}{{}^0\mathrm{F}^1_{-2}} - \eta\right]$$

Where η is the reduced chemical potential $\eta=u/\kappa_BT$, κ_B is the Boltzmann constant, e is the electron charge.

The carrier concentration $p_L$of light-mass valence band:

$$p_L = \frac{(2m^*\kappa_BT)^{3/2}}{3\pi^2\hbar^3}\ {}^0F_0^{3/2}$$

Where m^* is the density of state effective mass taking into account band degeneracy, ħ is the reduced Plank's constant, T is the absolute temperature.

The mobility μ_L of light-mass valence band:

$$\mu_L = \frac{2\pi\hbar^4eC_l}{m^*_I(2m^*_b\kappa_BT)^{3/2}\mathrm{E}^2_{\mathrm{def}}}\frac{3\ {}^0F^1_{-2}}{{}^0F_0^{3/2}}$$

Where C_l (C_l =5.82×10[10] Pa for SnTe[3]) is a parameter determined by the combination of the elastic constant (C_l =υ_l^2 d, where υ_l is the longitudinal speed of sound, d is the density), E_{def} is a combination of deformation potentials for multivalley systems[4, 5], which describes the carrier scattering strength by acoustic phonons.

The Hall factor $A_L$of light-mass valence band ($p=A_Lp_H=A_L/eR_{HL}$):

$$A_L = \frac{3K(K+2)}{(2K+1)^2}\frac{{}^0F^{1/2}_{-4}\ {}^0F^{3/2}_0}{({}^0F^1_{-2})^2}$$

$K=m_{\parallel}^*/m_{\perp}^*$ (K=4, assumed T independent[3]). Due to the anisotropy of both conduction and valence bands at the L point, the inertial effective mass m_I^*, and the density of states effective mass m^* are governed by the effective band mass of a single pocket along two directions $m_{\parallel}^*$ and $m_{\perp}^*$:

$$m_I^* = 3(\frac{2}{m_{\perp}^*}+\frac{1}{m_{\parallel}^*})^{-1},\ m^* = N_V^{2/3}m_b^* = N_V^{2/3}(m_{\perp}^{*2}m_{\parallel}^*)^{1/3}.$$

Where N_V is the band degeneracy (N_{V1}=4 for the light-mass valence band, N_{V2}=12 for the heavy-mass valence band of SnTe[6]).

And the Lorenz number L_L of light-mass valence band:

$$L_L = \left(\frac{\kappa_B}{e}\right)^2\left[\frac{{}^2F^1_{-2}}{{}^0F^1_{-2}} - \left(\frac{{}^1F^1_{-2}}{{}^0F^1_{-2}}\right)^2\right]$$

In the equations above the integral ${}^{n}F_{l}^{m}$ is defined by

$$ {}^{n}F_{l}^{m} = \int_{0}^{\infty} \left(-\frac{\partial f}{\partial \varepsilon}\right) \varepsilon^{n} (\varepsilon + \alpha\varepsilon^{2})^{m} [(1 + 2\alpha\varepsilon)^{2} + 2]^{l/2} d\varepsilon $$

Within the single parabolic model, the transport parameters of heavy-mass valence band are expressed as follows:

$$ S_H = \frac{\kappa}{e}\left[\frac{2F_1}{F_0} - (\eta - \Delta)\right] $$

Where F_0 and F_1 are Fermi integrals and Δ is the reduced energy difference between the bottoms of the two bands,

$$ \Delta = E_V/\kappa T $$

The carrier concentration p_H of the heavy-mass valence band:

$$ p_H = 4\pi \left(\frac{2m^{*}\kappa T}{h^2}\right)^{3/2} F_{1/2}(\eta - \Delta) $$

The mobility μ_H of the heavy-mass valence band:

$$ \mu_H = \mu_0 \frac{F_{-1/2}}{2F_0} $$

The Hall factor A_H ($p=A_H p_H=A_H/eR_{HH}$) of the heavy-mass valence band:

$$ A_H = \frac{3}{2} F_{1/2} \frac{F_{-1/2}}{2F_0^2} $$

And the Lorenz number L_H of the heavy-mass valence band:

$$ L_H = \frac{\kappa^2}{e^2} \frac{3F_0F_2 - 4F_1^2}{F_0^2} $$

According to the two band model, the carrier concentration p:

$$ \mathrm{p} = p_L + p_H $$

The Hall coefficient R_H:

$$ R_H = \frac{\sigma_L^2 R_{HL} + \sigma_H^2 R_{HH}}{(\sigma_L + \sigma_H)^2} $$

The Hall mobility μ_H:

$$ \mu_H = R_H \sigma $$

The effective mass and deformation potential were fit for the light band first, using low carrier concentration results, and then the heavy band parameters were adjusted. We allowed the effective mass for the light and heavy band and the band offset to vary as a function of temperature such that we obtained the best fit to experimental data. In this work, the number of degenerate valleys was assumed to be 4 and 12 for light and heavy bands respectively following similar results from PbTe[7]. Lattice thermal conductivity was calculated using the 2-band Lorenz number for the Iodine doped samples which gave consistent results among the different samples. For the p-doped samples, however, a Single Kane band model was used to calculate the Lorenz number.

At 300 K, the density of states effective mass of light band (m_L^{*}) and heavy band (m_H^{*}) are fitted as 0.14 m_e and 1.7 m_e, respectively. They linearly increase with temperature, as shown in Figure 2S (a) and (b). The reduced energy difference between the bottoms of the two bands ΔE is 0.4 eV at 300 K and decrease with temperature for SnTe.

The lattice thermal conductivity of the SnTe system was calculated as shown in Figure 3e for I-doped samples using a two band model to estimate the Lorentz number. In the case of $SnTe_{1+x}$ and $Sn_{1-x}Gd_xTe$, the calculation lead to a much larger spread in κ_L values (±50%), we find that the

differences are less large when a single band model is used. In addition, the two band model resulted in additional deviation. While we believe that the I-doped lattice thermal conductivity is more correct, we have included the lattice thermal conductivites of Te and Gd doped samples (estimated using a single Kane band model) in Figure S3.

In addition to the transport properties shown in the main text, we have included the calculated temperature dependent power factor in Figure S4. We can see that the power factor is enhanced slightly in the I-doped sample, but the zT enhancement should also be reflected by the lower electronic thermal conductivity.

In the main text, not all of the sample's transport properties have been shown in order to more clearly show trends. We have included results from other synthesized samples in Figure S5 which represent the temperature dependent results for samples in Table S1.

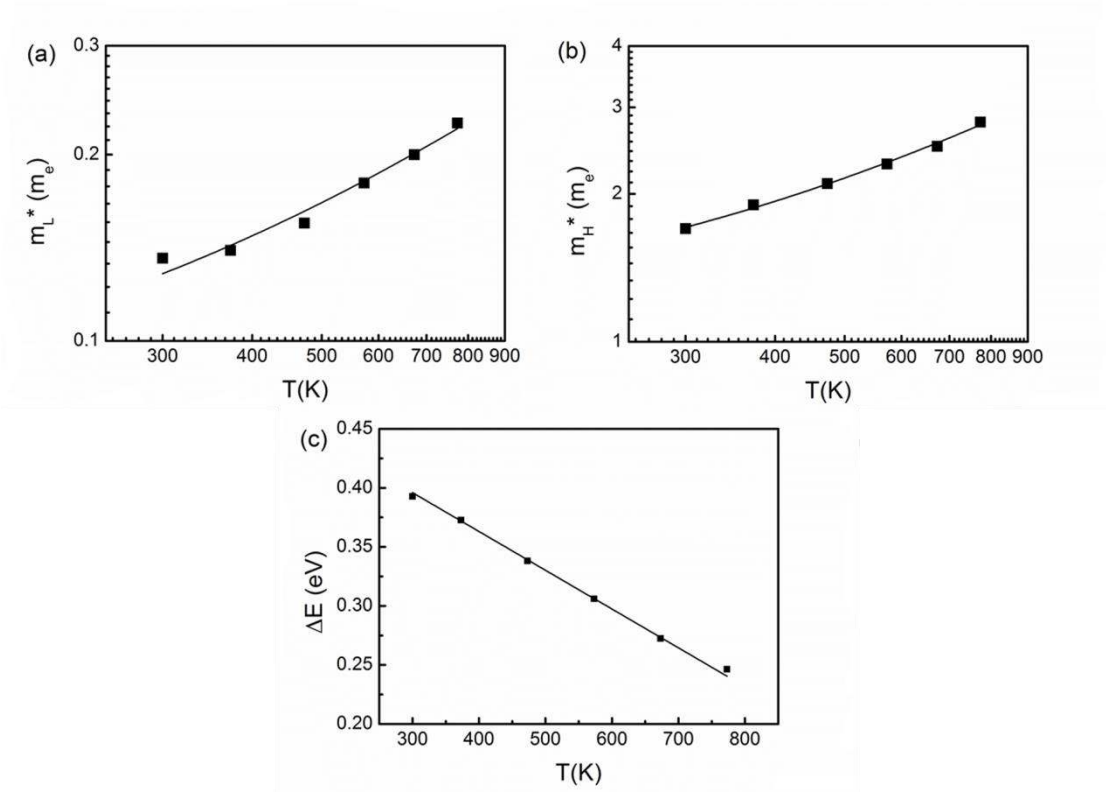

Figure S2. Density of states effective mass of: (a) light band (m_L^*), (b) heavy band (m_H^*), and (c) reduced energy difference between the bottoms of the two bands (ΔE).

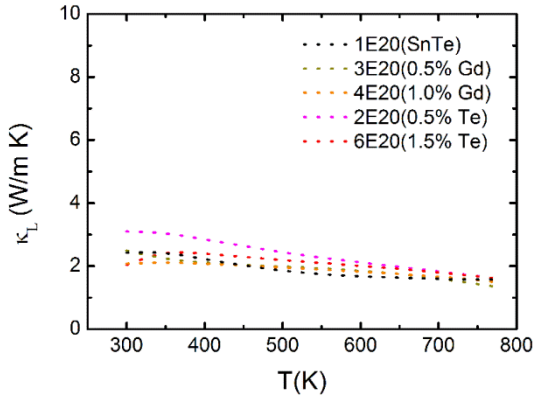

Figure S3. The lattice thermal conductivity of $SnTe_{1+y}$ and $Gd_zSn_{1-z}Te$. (The Lorenz number was calculated by using SKB model)

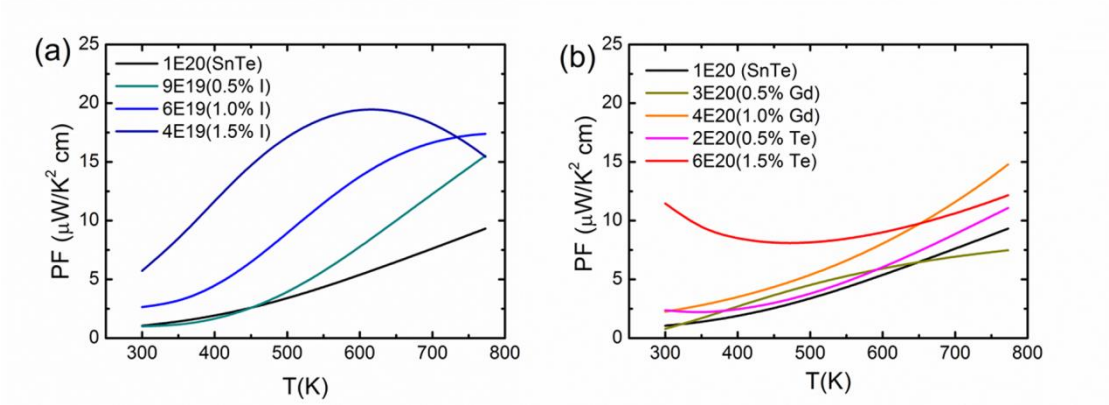

Figure S4 The power factor of SnTe, $SnTe_{1+y}$, $SnTe_{1-x}I_x$, and $Gd_zSn_{1-z}Te$.

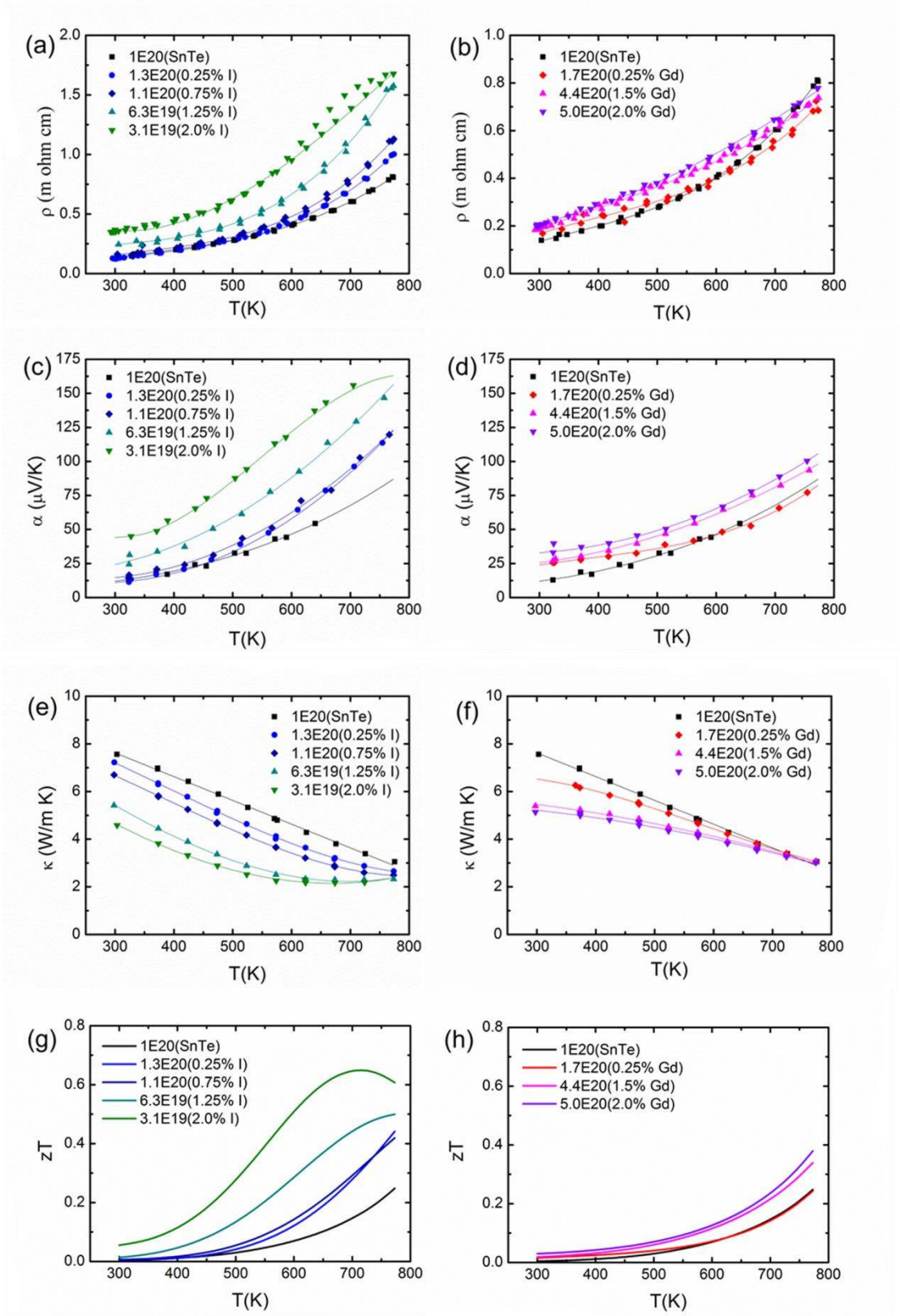

Figure S5 Thermoelectric transport properties for various SnTe samples: a) resistivity of SnTe and $SnTe_{1-x}I_x$, b) resistivity of SnTe, and $Gd_zSn_{1-z}Te$, c) Seebeck of SnTe and $SnTe_{1-x}I_x$, d) Seebeck of SnTe and $Gd_zSn_{1-z}Te$, e) thermal conductivity of SnTe and $SnTe_{1-x}I_x$, f) thermal conductivity of SnTe and $Gd_zSn_{1-z}Te$, g) zT of SnTe and $SnTe_{1-x}I_x$, h) zT of SnTe and $Gd_zSn_{1-z}Te$.

1. Y. Tung and M. L. Cohen, *Physical Review*, 1969, **180**, 823-826.
2. S. Rabii, *Physical Review*, 1969, **182**, 821.
3. T. Seddon, S. C. Gupta and G. A. Saunders, *Solid State Communications*, 1976, **20**, 69-72.
4. C. Herring and E. Vogt, *Physical Review*, 1956, **101**, 944-961.
5. Y. I. Ravich, B. A. Efimova and Tamarche.Vi, *Physica Status Solidi B-Basic Research*, 1971, **43**, 453-&.
6. L. M. Rogers, *J Phys D Appl Phys*, 1968, **1**, 1067-1070.
7. L. M. Rogers, *Journal of Physics D-Applied Physics*, 1968, **1**, 845-&.